ELSEVIER

Journal of Molecular Catalysis A: Chemical 167 (2001) 181–190

JOURNAL OF MOLECULAR CATALYSIS A: CHEMICAL

www.elsevier.com/locate/molcata

NO–CO reaction kinetics on Pd/MgO model catalysts: morphology and support effects

Laurent Piccolo[1], Claude R. Henry*

CRMC2 (Associated to the Universities of Aix-Marseille II and III)-CNRS, Campus de Luminy, case 913, 13288 Marseille Cedex 09, France

Received 4 April 2000

Abstract

The NO–CO reaction kinetics has been studied on Pd/MgO (1 0 0) model catalysts at low pressure by a pulsed molecular beam technique. The model catalysts have been prepared by epitaxial growth of metal clusters in UHV on cleaved MgO single crystals. Three samples with mean clusters sizes of 2.8, 6.9 and 15.6 nm have been studied. The reaction products are mainly N_2 and CO_2. The steady-state reaction rate has been measured between 150 and 400°C at low pressures (10^{-9}–10^{-6} Torr). The rate limiting step for the reaction is the dissociation of NO at low temperature and the adsorption of CO at high temperature. The reaction probability of NO has been accurately determined, taking into account the reverse spillover of NO from the MgO support towards the Pd particles. It is shown that in these conditions the turnover number is not an appropriate parameter to determine the intrinsic effect of particle size. The intrinsic activity depends not only on particle size but also on particle shape. The medium sized particles exhibiting mainly (1 1 1) facets are found to be more active. The largest particles, which exhibit principally (1 0 0) facets, are less active.

Keywords: Pulsed molecular beam technique; NO–CO reaction kinetics; Turnover number; Supported model catalyst

1. Introduction

The reduction of NO by CO is a very important reaction for air depollution, in particular, in the car exhaust three-way catalysts [1]. These catalysts remove toxic CO and nitrogen oxides and completely oxidize the unburnt hydrocarbons. The catalysts contain a mixture of Pt and Rh and sometimes Pd is added. The support is alumina, doped by other oxides (ceria and lanthania). Rh is used because of its very high activity for reducing NO to N_2. Pt (or Pd) is very efficient in the oxidation of CO. However, the price of Rh is very high and it is advantageous to replace this metal by less expensive ones. Despite its smaller activity in the NO reduction, Pd could provide an alternative to Rh. This explains the large number of studies concerning the CO + NO reaction on Pd in the recent years [2–14]. Extensive work has been performed in the group of Goodman [5–9]. They have shown that the activity for this reaction decreases when the structure of the Pd surface becomes more open. On Pd model catalysts, the activity drops when cluster size decreases. On powder catalysts, the activity also decreases with clusters size but it is far lower (for the same cluster size) than on planar supported (on the same alumina support) model catalysts. Two factors have been proposed to explain the decrease of the activity when the co-ordination of Pd surface atoms decreases (or when the cluster size

* Corresponding author. Tel.: +33-6-62922832; fax: +33-491-41-8916.
E-mail address: henry@crmc2.univ-mrs.fr (C.R. Henry).
[1] Present address: DSM/DRECAM/SRSIM, CEA Saclay-bât. 462, 91191 Gif-sur-Yvette Cedex, France.

1381-1169/01/$ – see front matter
PII: S1381-1169(00)00505-7

decreases). The first one is the higher NO concentration (relative to CO) on the (1 1 1) surface than on the (1 0 0), which favors the reaction for the more compact surface (under actual reaction conditions) [7]. The second factor is the presence of a strongly adsorbed N_{ad} species that desorbs at a temperature (560–600 K) higher than CO or NO, then this nitrogen species tends to cover the surface and acts as a poison for the reaction. The relative proportion of this strongly bound N_{ad} increases when the Pd surface becomes more open or when cluster size decreases (the proportion of low co-ordinated sites increasing) [9]. Under these conditions, it is assumed that the rate-limiting step of the reaction is the recombination of adsorbed nitrogen atoms to give N_2 molecules, and not the dissociation of NO as generally admitted on Rh (at moderate pressures and not too high a temperature) [15]. The much smaller activity of powder catalysts is more difficult to explain.

In order to get more insight into the origin of the size effects in the CO–NO reaction, we have recently started a detailed study of this reaction on Pd/MgO (1 0 0) model catalysts. To access to the elementary reaction steps involved in this reaction we have used a pulsed molecular beam technique, which allows to get, from isothermal kinetics, the elementary reaction steps and the corresponding energetic parameters. We have successively studied the interaction of NO with the clean MgO (1 0 0) surface and with the surface covered by Pd clusters [16]. Some years ago, we had investigated the interaction of CO with the same system [17–19]. Then, the reaction itself was studied both under transient and steady-state conditions. The first results and the characterization of the Pd clusters have been presented elsewhere [20]. In this paper we present new results elucidating the rate-limiting steps of the reaction at low and high temperatures (at low pressure) and we explain the role of the support and of the cluster morphology on the reaction rate.

2. Experimental

The Pd clusters were prepared by condensing a calibrated (2×10^{13} atoms/cm^2) atomic beam of Pd on a clean MgO (1 0 0) surface at high temperature (400°C). The clean MgO (1 0 0) surfaces were obtained by cleavage under UHV or by air cleavage followed by an in situ annealing at 700°C for 5 h. The cleanness of the MgO substrates was checked by Auger electron spectroscopy. During growth, the pressure in the vacuum chamber remained in the 10^{-9} Torr range, which is essential to get clean Pd clusters. After the end of the experiments, the sample was covered by a thin carbon film which was subsequently floated in dilute hydrochloric acid (6%) and mounted on electron microscopy copper grids. The metal clusters where observed in a JEOL 2000 FX electron microscope.

For the reactivity measurements, a molecular beam of NO, generated by supersonic expansion, was directed towards the sample. The beam could be modulated by a computer-controlled shutter. For these experiments the NO beam had a constant intensity (1.9×10^{13} molecules/cm^2) on the sample (equivalent to a pressure of 5.2×10^{-8} Torr). During the experiments, in the presence of the NO beam, the background pressure of NO was 1.9×10^{-10} Torr, then the reaction with background NO was neglected. An isotropic pressure of isotopically labeled ^{13}CO was controlled by a leak valve. The molecules desorbed (or scattered) from the sample were detected by a quadrupole mass spectrometer. The mass spectrometer was computer controlled and synchronized with the beam chopper. More details on the experimental assembly can be found in a previous paper [18].

3. Characterization of the Pd clusters

The main advantage in using supported model catalysts obtained by epitaxial growth on oxide single crystals is to get uniform distributions of metal particles sizes, having well defined shapes. This is an essential feature to study the role of the particle size and morphology in the kinetics of a catalytic reaction [21]. We have shown in previous TEM studies that large (10 nm or more) Pd particles grown at high temperature have a truncated octahedron shape exhibiting mainly (1 1 1) facets [22]. Small Pd clusters (2–7 nm) have the shape of a truncated square pyramid exhibiting also a majority of (1 1 1) facets [23,24]. When the density of clusters is very large and for long deposition times, coalescence occurs during growth, resulting in flat particles presenting now a majority of (1 0 0) facets [23]. For the following results, three samples have been used, presenting mean sizes of 2.8, 6.9

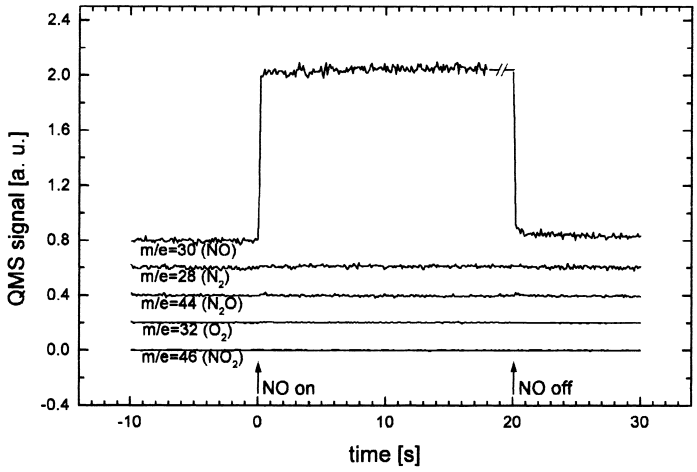

Fig. 1. Time evolution of mass spectrometer signals corresponding to NO, N_2, N_2O, O_2 and NO_2 scattering or desorbing from a clean MgO (1 0 0) surface during an incident pulse of NO, $T_s = 232^\circ$C.

and 15.6 nm with size dispersions of 23, 27 and 24%, respectively. More details on the characterization of these Pd particles can be found elsewhere [20,25]. Only the largest particles (sample with a mean size of 15.6 nm) showed a very large fraction of coalesced particles, which exhibited mainly (1 0 0) facets.

4. NO adsorption

We have first studied the interaction of an NO molecular beam with a clean MgO (1 0 0) surface. Fig. 1 shows the signal detected by the mass spectrometer for the masses 28, 30, 32, 44, 46 corresponding, respectively, to N_2, NO, O_2, N_2O and NO_2, in response to an incident pulse of NO at a sample temperature of 232°C. No signals except those of NO are detected, proving that no reaction had occurred on the MgO surface, as expected on a clean MgO surface presenting a very low density of defects [26]. Moreover, the NO signal is not demodulated (also at *RT*), which means that the residence time of the NO molecules on the MgO surface is much smaller than the rise time of the incident pulses (20 ms). These results exclude the possibility of NO chemisorption. They are in agreement with recent TPD experiments [27] of NO on MgO (1 0 0), showing a desorption energy of 5.1 kcal/mol, characteristic for physisorption. Angular distributions of NO were peaked near the specular direction, indicating the presence of quasi-elastic reflection of NO. A quantitative analysis of the angular distribution has shown that it can be decomposed in a cosine component and in a lobular one [16]. The amplitude of the cosine part, which is due to NO desorbing from a physisorbed state, gives the adsorption probability (0.56 ± 0.03) on an UHV-cleaved MgO surface [16].

After deposition of the Pd clusters, the mass spectrometer shows the presence of N_2 and a very weak signal of N_2O. In Fig. 2, one can see an NO pulse and an N_2 pulse desorbed simultaneously at 232°C from a collection of 2.8 nm Pd clusters. Looking at this figure, three remarks can be immediately made: (i) the NO signal is demodulated and the residence time is of the order of several seconds, indicating a chemisorption state; (ii) the presence of N_2 indicates that some CO molecules dissociate on the Pd clusters; (iii) the area of the difference between the incident square pulse and the re-emitted NO signal during the first half of the pulse (A_a) represents the amount of NO that has been adsorbed on Pd. The area under the emitted NO signal during the second half of the pulse (A_d) represents the amount of NO desorbed molecularly from Pd. A_a is larger than A_d, indicating that part of the adsorbed NO is not re-emitted as NO molecules. These observations are explained by the chemisorption of NO molecules and the dissociation of some of them. The dissociation efficiency has been measured

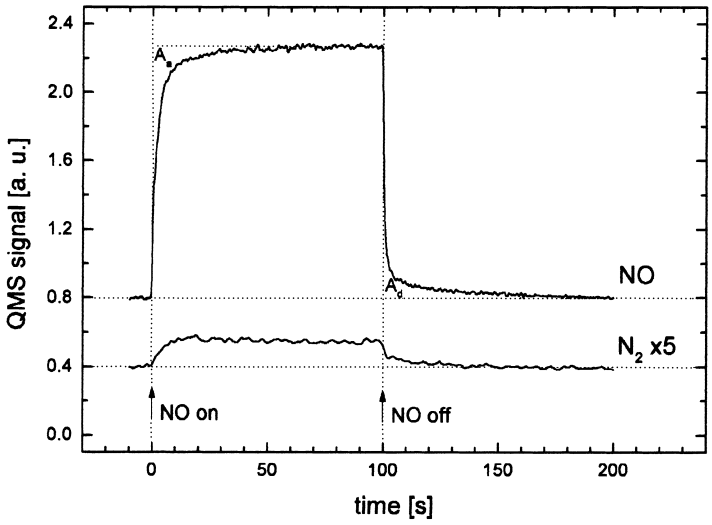

Fig. 2. Re-emitted NO and emitted N_2 signals from 2.8 nm Pd clusters at 232°C in response to an NO pulse. A_a and A_d correspond to the amount of NO molecules adsorbed during the NO pulse and to the amount of NO desorbed after the pulse, respectively.

by $(A_a - A_d)/A_a$ [16]. The measurements have shown that already at 170°C the dissociation is not negligible and that it increases up to 80% at 430°C [16] (see also Fig. 8). It is important to note that the above defined dissociation efficiency is not the dissociation probability of an incident molecule. It represents the average dissociation rate of adsorbed molecules during an NO pulse. The probability that an NO molecule impinging on the Pd clusters dissociates is much smaller. During a pulse of 100 s, the average value is around 5%. This value is in agreement with the desorbing flux of dinitrogen.

A close inspection of Fig. 2 shows that the NO signal evolves with two kinetics: a sharp variation when the beam is switched on or off, followed by a slow variation. The first kinetics corresponds to NO molecules reflected or desorbed from the MgO substrate, while the slow kinetics corresponds to the NO molecules desorbed from the Pd clusters. Indeed, in this case, the life-time of the NO molecules on the MgO substrate is much lower than the rise time of the NO pulses (20 ms), while the life time of the NO molecules on the Pd clusters is of the order of one second. Then it is possible to separate the NO molecules desorbing from the support from those desorbing from the Pd clusters. The amplitude of the slow variation divided by the incident flux represents the probability for an incident molecule to be chemisorbed on Pd at zero coverage. This (global) adsorption probability is equal or larger than the fraction of the substrate covered by the Pd clusters, and it increases when temperature decreases [16]. As more molecules adsorb on the Pd than by the direct flux impinging on the clusters it is obvious that some NO adsorbs on the Pd clusters via another route. In fact, part of the NO physisorbed on the MgO support diffuses toward the Pd clusters, where it becomes chemisorbed. The same effect has been already observed for CO on MgO and quantitatively modeled [17]. We will see later that this effect plays an important role on the reaction kinetics, as already observed in the CO oxidation on Pd supported on mica [28], MgO [29] and sapphire [30–32]. In Fig. 3, the ratio of the total NO flux joining the Pd clusters to the direct impinging flux obtained from the adsorption kinetics measurements has been plotted as a function of the substrate temperature and for different cluster sizes. It is remarkable that for 2.8 nm Pd clusters the total flux can be as large as six times the direct flux. At low temperatures, the total flux reaches saturation when all the capture zones around the clusters overlap [17].

The desorption energy has been measured using a periodic modulation of the NO beam in order to have small variations of the NO coverage. This is necessary, since the desorption energy strongly depends on

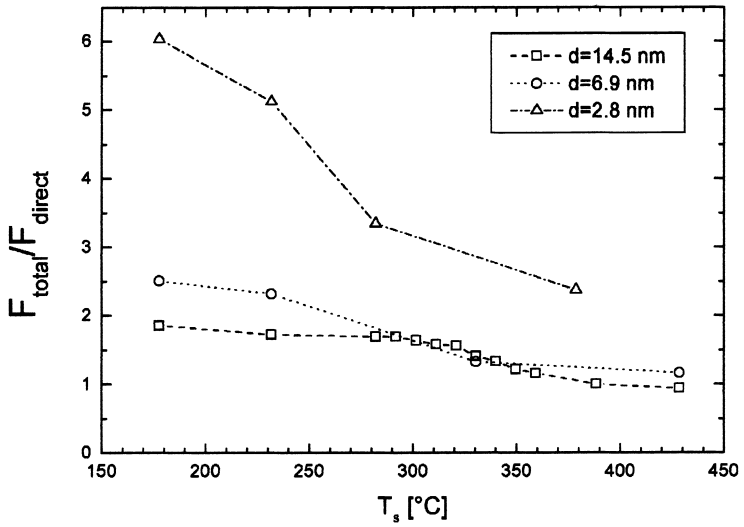

Fig. 3. Ratio of the total NO flux reaching the Pd clusters to the direct flux as a function of the substrate temperature and for different cluster sizes.

the NO coverage, resulting in non-linear desorption kinetics. These measurements have given a desorption energy of 32 kcal/mol for coverages between 0.01 and 0.1 [16].

5. CO adsorption

The adsorption of CO on Pd clusters supported on MgO (1 0 0) has been previously studied by the same molecular beam techniques [17–19]. Here, we only summarize the main results. CO does not react with the MgO surfaces. As for NO, it is partially reflected and partially physisorbed. The adsorption probability (0.50) is smaller than for NO due to a weaker interaction [17]. CO physisorbed on the MgO substrate is also a precursor state for chemisorption on the Pd clusters [17]. CO does not dissociates on the Pd clusters (grown at high temperatures, thus, presenting well faceted shapes) [18,19]. For clusters larger than 5 nm the adsorption energy at low coverages (a few percents of a monolayer) is nearly constant and equal to 30 kcal/mol, while for smaller clusters the adsorption energy increases when cluster size decreases [19]. This increase of the adsorption energy has been explained by a stronger adsorption on the low-co-ordinate Pd edge atoms [21].

6. NO–CO reaction

The NO–CO reaction has been studied by impinging, at a given temperature, pulses of NO (generally 100 s long) on the sample, which is also exposed to a constant isotropic pressure of ^{13}CO. During the experiments, the NO, N_2, N_2O and $^{13}CO_2$ molecules desorbing from the sample are recorded by the mass-spectrometer. Fig. 4 displays the rate of desorption of the reaction products at the end of the pulse (which is assumed to correspond to the steady-state) for 2.8 nm particles. The major products are CO_2 and N_2 but a small production of N_2O is observed between 200 and 300°C. Below 300°C the reaction is compatible with the global equation (we neglect the production of nitrous oxide)

$$CO + NO \rightarrow CO_2 + \tfrac{1}{2}N_2 \quad (1)$$

At temperatures higher than 300°C, less CO_2 is produced than expected from the stoichiometric Eq. (1). The temperature variations of the two main products show a volcano plot with a maximum reaction rate near 250°C (for the considered conditions). The reaction is limited at low and high temperatures by two different reaction steps. The rate-limiting step (RLS) at low temperature is the dissociation of NO because of a too large surface coverage, as in the case of Rh [15].

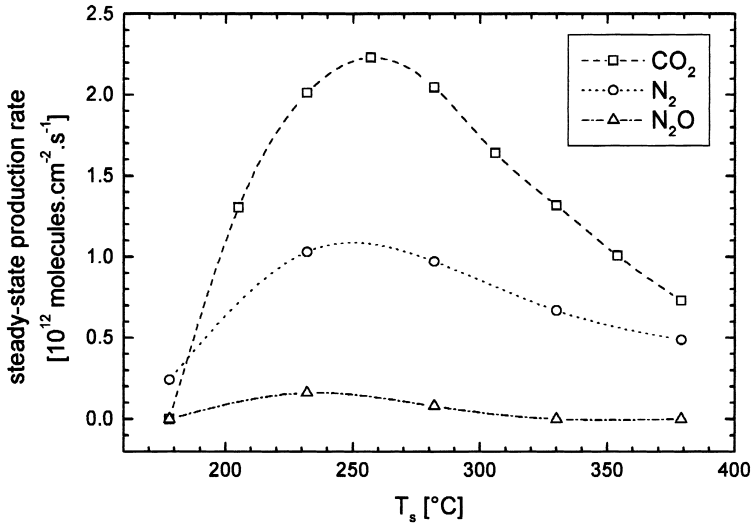

Fig. 4. Steady-state production rate of CO_2, N_2 and N_2O as a function of temperature for 2.8 nm Pd clusters and a partial pressure of CO of 2.0×10^{-8} Torr. The equivalent pressure in the NO beam is 5.2×10^{-8} Torr.

This explanation is supported by several observations. First, the associative desorption of adsorbed nitrogen is not suspected to limit the reaction in this regime, because the transients of N_2 production follow nearly the same kinetics as the CO_2 and NO desorptions, implying that this step is fast [25]. The second argument is given by Fig. 5. In this figure the NO transients are recorded during the reaction ($P_{CO} = 5 \times 10^{-8}$ Torr) and in the absence of CO, at 232°C and 282°C. The area under the desorbed NO curve after beam closing represents the quantity of molecularly adsorbed NO at steady-state. At low temperature, some NO is molecularly adsorbed during the reaction, while no molecular NO is adsorbed during the reaction in the high temperature regime. Thus, at high temperature there is no limitation for NO dissociation, while at low temperature NO dissociation is limited by too high a coverage. The RLS in the high temperature regime is the adsorption of CO as clearly proven by Fig. 6. In this figure, the steady-state production of CO_2 is plotted as a function of the sample temperature for different CO pressures. At low temperature the reaction rate is independent of the CO pressure (if the CO pressure becomes too high, it is no longer true, because in this case the CO coverage limits the NO adsorption and dissociation). However, at high temperature the reac-

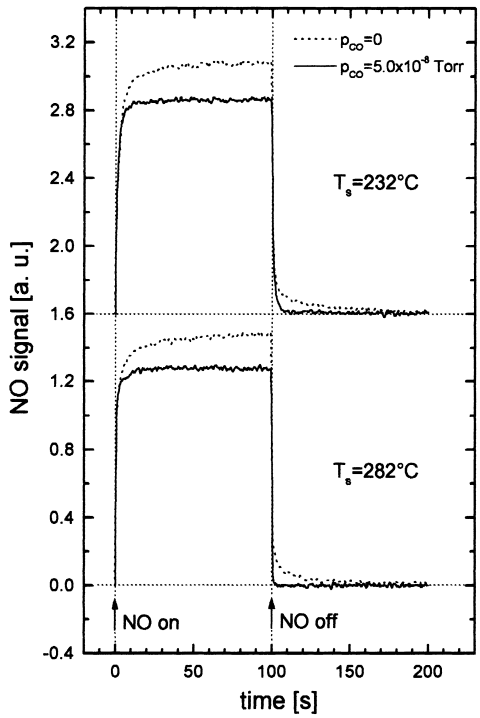

Fig. 5. Re-emitted NO pulses in the presence of a partial pressure of CO equal to 5.0×10^{-8} Torr (solid lines) and without CO (dotted lines) at 232 and 282°C for 2.8 nm Pd clusters.

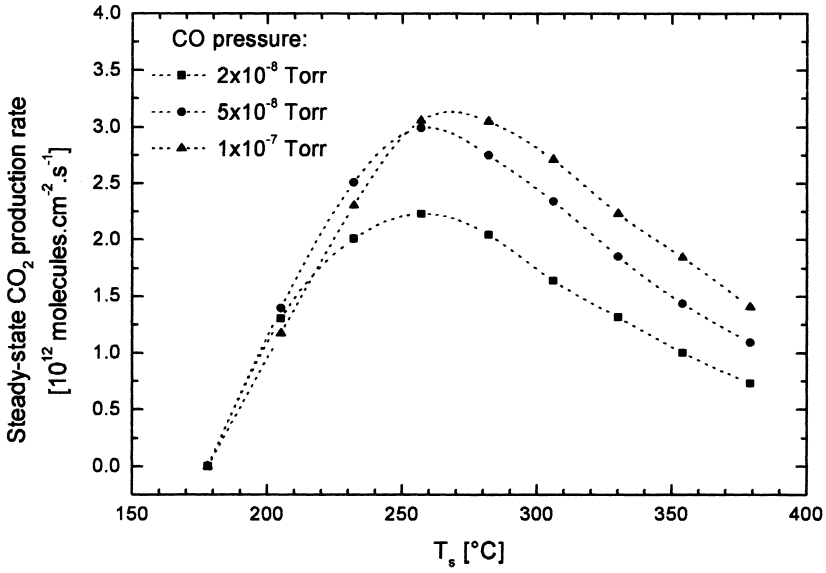

Fig. 6. Steady-state production of CO_2 as a function of sample temperature at different CO partial pressures for 2.8 nm Pd clusters.

tion rate increases with the CO pressure. In the high temperature regime there is not enough CO to remove all the adsorbed oxygen resulting from the NO dissociation. For the same reason, the production rate of CO_2 is smaller than two times the production rate of N_2 (see Eq. (1)).

The effect of the particle size has been already previously addressed [20]. It was shown that the turnover number (TON: number of molecules produced per second and per Pd surface atom) increased when cluster size decreased (between 15.6 and 2.8 nm, the TON of CO_2, at the temperature, where it is maximum, increases from 0.003 to 0.0095 s^{-1}) [20]. If the TON is a significant parameter to compare the activity of different single crystals, it is not obvious that it is appropriate to compare the intrinsic activity of samples with different cluster sizes. In fact, we have seen in Section 4 that the net adsorption rate of NO on the Pd clusters depends on cluster size (and on cluster density) because of the capture of NO physisorbed on the substrate (this phenomenon is sometimes called reverse spillover). Briefly, it is possible to define a capture zone around each Pd cluster, where all the NO molecules which become physisorbed will be captured by the Pd clusters, via surface diffusion [17]. The width of these capture zones depends on the substrate temperature. Then, at a given temperature the quantity of molecules joining the clusters, by this mechanism, will increase by decreasing cluster size. Moreover, when the capture zones overlap several cluster will compete for the capture of the diffusing NO molecules, then the flux of NO molecules joining the clusters by surface diffusion will decrease by increasing the density of clusters. For the samples used in the present study the effect of cluster size is dominant i.e. for a given equivalent pressure in the NO beam the net adsorption rate of NO is larger on smaller clusters (see Fig. 3). Therefore, to have insight into the intrinsic size effect for the reaction, it is more suitable to measure the reaction probability of NO, which is equal to the probability for a NO molecule arriving on a Pd cluster to react. The consumption rate of NO molecules by the reaction (at steady-state) is given by the difference between the NO impinging flux and the NO desorbing flux during the reaction. The net adsorption flux of NO on the Pd clusters has been measured in the NO adsorption–desorption experiments (see Fig. 3). Then, the reaction probability of NO can be measured accurately. Fig. 7 shows the NO reaction probability as a function of the sample temperature for three cluster sizes (2.8, 6.9 and 15.6 nm). Now the variations between the different samples are not as large as for the

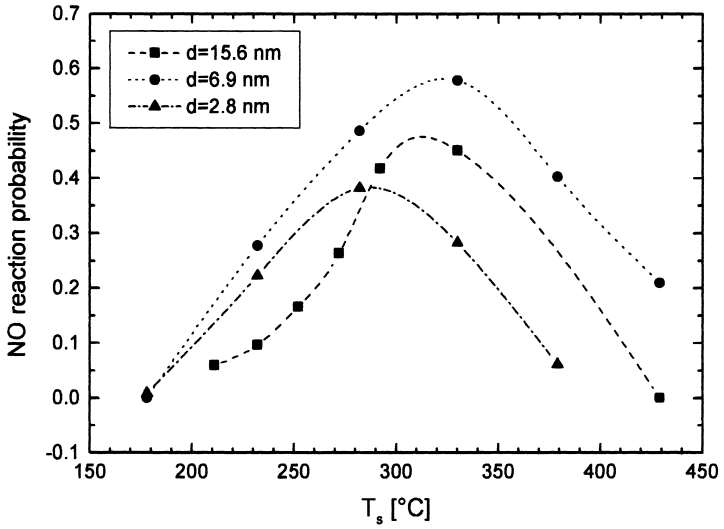

Fig. 7. NO reaction probability as a function of sample temperature for different Pd cluster sizes, $P_{CO} = 5.0 \times 10^{-8}$ Torr.

TON, but more surprising is that the medium sized clusters are the more active. In fact, this result can be understood easily in the low temperature regime (i.e. below 250°C). We have seen that in this regime the reaction rate is limited by the NO dissociation. Fig. 8 displays the dissociation efficiency of NO as a function of the sample temperature for the three studied samples. We see that, in the temperature range 170–280°C, corresponding to the low-temperature regime of the reaction, the dissociation efficiency follows the same trend as the NO reaction probability. However, how can we understand that the medium sized (6.9 nm) particles are the more active and the largest ones (15.6 nm) the least active? These differences are probably due to the shape of the Pd particles. The largest particles have coalesced and expose mainly (1 0 0) facets while the

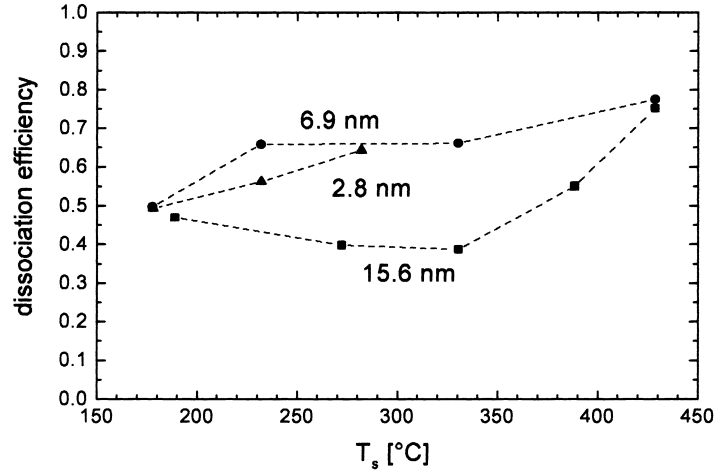

Fig. 8. Dissociation efficiency of NO as a function of substrate temperature for different cluster sizes (at zero CO pressure). The dissociation efficiency represents the average proportion of NO molecules dissociated, among the NO molecules adsorbed, during the NO pulse in stationary conditions (the irreversible dissociation during the first NO pulse on the fresh sample is not taken into account [16]).

medium sized particles present mainly (1 1 1) facets [20]. From the work of Goodman's group on Pd single crystals, (1 1 1) planes are much more active than (1 0 0) planes for the NO–CO reaction [9], clarifying why the largest particles are less active. Now, why the smallest particles are between the two other sizes? A possible explanation is that the small particles, which also expose (1 1 1) facets [24], present a high proportion of step edges. These low-co-ordinated sites would be little active (or inactive) if we extrapolate the observation that, when the co-ordination of the Pd atoms in a facet decreases, the activity of the facet decreases [8]. The fact that in our observations the increase of the NO dissociation is correlated with the increase of activity seems contradictory with the observation of a greater dissociation and a smaller activity by decreasing particle size [9]. However, as pointed out by Rainer et al. [9], the dissociation of NO leads to two types of nitrogen adsorbed species: a weakly bound nitrogen species desorbing associatively below 500 K, and a strongly bound one desorbing associatively near 600 K. The proportion of the strongly bound nitrogen increases when surface structure becomes more open or when particle size decreases. It has been also shown that this strongly bound species is a poison for the reaction [9]. In our experiments, the activity for the NO–CO reaction is correlated with the reversible dissociation of NO. We associate the nitrogen atoms coming from this reversible dissociation to the weakly bound nitrogen species, which are active for the reaction. However, during the first adsorption pulse of NO on a fresh sample, we observed a very large dissociation, which is partly irreversible [16]. In other words, part of the dissociated nitrogen is not able to desorb at the reaction temperature. This irreversibly adsorbed nitrogen is assigned to the strongly bound nitrogen species described in the work of Goodman's group. Then the decrease in activity, observed on the more open surfaces or on the smallest particles should be due to a decrease of the available sites for the NO dissociation, due to poisoning by strongly bound nitrogen atoms.

Anyway, a correlation between cluster size and activity is only valid if the metal clusters have the same shape. In the present study, we have shown that 15.6 nm particles are less active than 6.9 and 2.8 nm particles because the large particles expose mainly (1 0 0) facets and the other ones mainly (1 1 1) facets.

7. Conclusion

The NO–CO reaction has been studied on Pd/MgO (1 0 0) model catalysts by molecular beam techniques. The rate-limiting step of the reaction at low temperature is NO dissociation, while at high temperature it is the CO adsorption. The TON is not an appropriate parameter to describe the intrinsic size effect because molecules physisorbed on the support increase, by reverse spillover, the effective flux of reactants reaching the metal clusters. The reaction probability of NO, which quantitatively takes this effect into account, has been measured, allowing the determination of the particle size effect for the reaction. From the three studied samples, the largest particles appear to be the less active because they expose mainly (1 0 0) facets, contrary to smaller clusters exhibiting mainly (1 1 1) facets. Between the smaller particles, the smallest are the less active (at low temperature), probably because of a higher proportion of edge sites.

Therefore, the study of cluster size effect in catalysis is complicated because, for a structure sensitive-reaction, the activity depends not only on the particle size (mainly through the amount of low co-ordinated sites) but also on the particle morphology, which has to be accurately determined. The characterization of the particle shape is feasible on planar model catalysts, but remains very difficult on industrial catalysts.

References

[1] K.C. Taylor, Catal. Rev. Sci. Eng. 35 (1993) 457.
[2] G. Xi, J. Bao, S. Chao, S. Li, J. Vac. Sci. Technol. A 10 (1992) 2351.
[3] A. Obuchi, S. Naito, T. Onishi, K. Tamaru, Surf. Sci. 122 (1982) 235.
[4] T. Yamada, I. Matsuo, J. Nakamura, M. Xie, H. Hirano, Y. Yamatsumoto, K.I. Tanaka, Surf. Sci. 231 (1990) 304.
[5] X. Xu, D.W. Goodman, Catal. Lett. 24 (1994) 31.
[6] X. Xu, P. Chen, D.W. Goodman, J. Phys. Chem. 98 (1994) 9242.
[7] S.M. Vesecky, P. Chen, X. Xu, D.W. Goodman, J. Vac. Sci. Technol. A 13 (1995) 1539.
[8] S.M. Vesecky, D.R. Rainer, D.W. Goodman, J. Vac. Sci. Technol. A 14 (1996) 1457.
[9] D.R. Rainer, S.M. Vesecky, M. Koranne, W.S. Oh, D.W. Goodman, J. Catal. 167 (1997) 234.
[10] M. Daté, H. Okuyama, N. Takagi, M. Nishijima, T. Aruga, Surf. Sci. 34 (1995) L1096.
[11] M. Daté, H. Okuyama, N. Takagi, M. Nishijima, T. Aruga, Surf. Sci. 350 (1996) 79.

[12] M. Valden, J. Aaltonen, E. Kuusisto, M. Pessa, C.J. Barnes, Surf. Sci. 307–309 (1994) 193.
[13] M. Hirsimäki, S. Suhonen, J. Pere, M. Valden, M. Pessa, Surf. Sci. 402–404 (1998) 187.
[14] I. Kobal, K. Kimura, Y. Ohno, T. Matsushima, Surf. Sci. 445 (2000) 472.
[15] V.P. Zhdanov, B. Kasemo, Surf. Sci. Rep. 29 (1997) 31.
[16] L. Piccolo, C.R. Henry, Surf. Sci. 452 (2000) 198.
[17] C.R. Henry, C. Chapon, C. Duriez, J. Chem. Phys. 95 (1991) 700.
[18] C. Duriez, C. Chapon, C.R. Henry, Surf. Sci. 253 (1991) 190.
[19] C.R. Henry, C. Chapon, C. Goyhenex, R. Monot, Surf. Sci. 272 (1992) 283.
[20] L. Piccolo, C.R. Henry, Appl. Surf. Sci. 164 (2000) 156.
[21] C.R. Henry, Surf. Sci. Rep. 31 (1998) 231.
[22] H. Graoui, S. Giorgio, C.R. Henry, Surf. Sci. 417 (1998) 350.
[23] C.R. Henry, C. Chapon, C. Duriez, S. Giorgio, Surf. Sci. 253 (1991) 177.
[24] S. Giorgio, C.R. Henry, C. Chapon, J.M. Pénisson, J. Cryst. Growth 100 (1990) 254.
[25] L. Piccolo, Thesis, Marseille, 1999.
[26] C. Duriez, C. Chapon, C.R. Henry, J.M. Rickard, Surf. Sci. 230 (1990) 123.
[27] R. Wichtendahl, M. Rodriguez-Rodrigo, U. Hartel, H. Kuhlenbeck, H.J. Freund, Phys. Stat. Sol. A 173 (1999) 93.
[28] V. Matolin, E. Gillet, Surf. Sci. 166 (1986) L115.
[29] C. Becker, C.R. Henry, Surf. Sci. 352–354 (1996) 457.
[30] F. Rumpf, H. Poppa, M. Boudart, Langmuir 4 (1988) 722.
[31] C.R. Henry, Surf. Sci. 223 (1989) 519.
[32] I. Stara, V. Nehasil, V. Matolin, Surf. Sci. 365 (1996) 69.